Journal of Materials Chemistry C

Accepted Manuscript

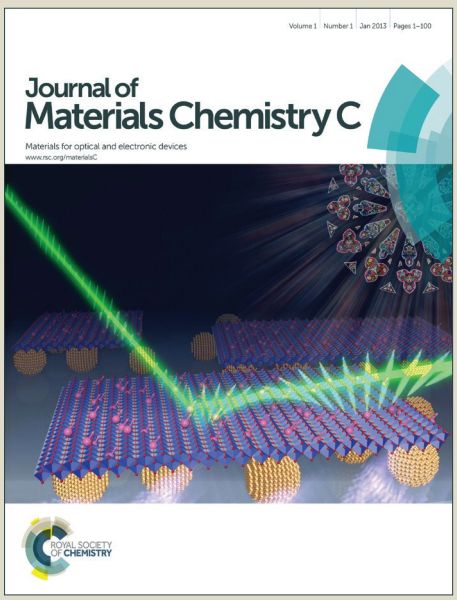

This is an *Accepted Manuscript*, which has been through the Royal Society of Chemistry peer review process and has been accepted for publication.

Accepted Manuscripts are published online shortly after acceptance, before technical editing, formatting and proof reading. Using this free service, authors can make their results available to the community, in citable form, before we publish the edited article. We will replace this *Accepted Manuscript* with the edited and formatted *Advance Article* as soon as it is available.

You can find more information about *Accepted Manuscripts* in the Information for Authors.

Please note that technical editing may introduce minor changes to the text and/or graphics, which may alter content. The journal's standard Terms & Conditions and the Ethical guidelines still apply. In no event shall the Royal Society of Chemistry be held responsible for any errors or omissions in this *Accepted Manuscript* or any consequences arising from the use of any information it contains.

ROYAL SOCIETY OF CHEMISTRY

www.rsc.org/materialsC

Journal Name RSCPublishing

ARTICLE

Cite this: DOI: 10.1039/x0xx00000x

Received 00th January 2014,
Accepted 00th January 2014

DOI: 10.1039/x0xx00000x

www.rsc.org/

Second-harmonic generation (SHG) and photoluminescence properties of noncentrosymmetric (NCS) layered perovskite solid solutions, $CsBi_{1-x}Eu_xNb_2O_7$ (x = 0, 0.1, and 0.2)

Hyung Gu Kim,[a] Jae Soo Yoo,[b] and Kang Min Ok[a,*]

Solid solutions of noncentrosymmetric (NCS) Dion-Jacobson phases, $CsBi_{1-x}Eu_xNb_2O_7$ (x = 0, 0.1, and 0.2) have been synthesized through standard solid-state reactions. Powder X-ray diffraction analysis suggests that the solid solutions crystallize in the NCS polar orthorhombic space group, $P2_1am$ (No. 26). $CsBi_{1-x}Eu_xNb_2O_7$ reveal layered perovskite structures that are composed of corner-shared distorted NbO_6 octahedra and the stereoacive A-cation, Bi^{3+}. Powder second-harmonic generating (SHG) measurements on the reported materials show that $CsBiNb_2O_7$, $CsBi_{0.9}Eu_{0.1}Nb_2O_7$, and $CsBi_{0.8}Eu_{0.2}Nb_2O_7$ possess SHG efficiencies of 50, 30, and 25 times that of α-SiO_2, respectively. The decrease in SHG for Eu^{3+}-doped compounds is attributable to the deficiency of net moment generating from the polyhedra of polarizable lone pair cation, Bi^{3+}. The stronger electric dipole transition bands compared to those of the magnetic dipole transitions in the photoluminescence emission spectra of $CsBi_{1-x}Eu_xNb_2O_7$ confirm the asymmetric coordination environment of Bi^{3+}/Eu^{3+} sites in the framework.

Introduction

Discovering novel materials exhibiting superior performance is one of the continuing challenges in materials chemistry. The fundamental approach to explore new functional materials comprises three important parts, *i.e.*, syntheses, structure determinations, and property measurements. The origin of peculiar properties of the materials is often explained through detailed structural analyses. This is particularly veracious for noncentrosymmetric (NCS) materials that can demonstrate diverse of great significance characteristics relating to both science and industry, such as piezoelectric, ferroelectric, multiferroic, pyroelectric, and nonlinear optical (NLO) properties.[1] In order to increase the possibility for functional NCS solid state materials, a number of strategies have been suggested thus far. Needless to say, one of the most successful methods for the synthesis of NCS mixed metal oxides must be combining both families of second-order Jahn-Teller (SOJT) distortive cations, namely, octahedrally coordinated d^0 transition metals and lone pair cations.[2] In addition, asymmetric π-orbital systems found in borates and d^{10} metal cations exhibiting polar displacement in the center of coordination moieties are considered to be other important NCS chromophores.[3] To design and develop functional NCS materials more effectively, a few critical factors such as structural origin of NCS properties and key elements contributing to a space group centricity should be adequately understood. Several factors controlling the macroscopic centricity in extended materials include the cation size, the hydrogen-bonding, and the framework flexibility effects.[4]

We have been very interested in layered perovskite materials exhibiting a variety of structure-driven properties such as ionic conductivity, magnetic properties, photocatalysis, superconductivity, ion-exchange, and intercalation.[5] To elucidate the structure-NCS property relationships, we have been exploring NCS layered perovskite phases.[6] One of the NCS layered perovskite oxides, $CsBiNb_2O_7$, classified as a member of Dion-Jacobson (DJ) series, has shown interesting NCS characteristics such as ferroelectricity and piezoelectricity attributed to its structural distortions.[7] Here, we present pure phase solid-state syntheses, structural refinements, spectroscopic characterization, second-harmonic generation (SHG) properties, a detailed study on the structural origin of the SHG behaviors, and photoluminescence properties of $CsBi_{1-x}Eu_xNb_2O_7$ (x = 0, 0.1, and 0.2) solid solutions. The added foreign cation, Eu^{3+}, not only indicates the asymmetric coordination sites for the associated SHG properties, but also promises important applications to novel phosphor materials.

Journal of Materials Chemistry C Accepted Manuscript

Experimental section

Synthesis

Polycrystalline samples of $CsBi_{1-x}Eu_xNb_2O_7$ (x = 0, 0.1, 0.2) were synthesized through standard solid-state reactions. Stoichiometric amounts of Cs_2CO_3 (25% excess, Alfa Aesar, 99%), Bi_2O_3 (Alfa Aesar, 99%), Eu_2O_3 (Alfa Aesar, 99.9%), and Nb_2O_5 (Alfa Aesar, 99.5%) were thoroughly mixed with agate mortars and pestles and pressed into pellets. The pellets were gradually heated to 1000 °C for 24 h and cooled down to room temperature rapidly at a rate of 10 °C min^{-1}. After grinding, the reaction products were washed with deionized water to remove excess cesium and dried in a drying oven at 100 °C for 8 h.

Powder X-ray diffraction (PXRD)

The PXRD data were collected on a Bruker D8-Advance diffractometer using Cu Kα radiation at room temperature with 40 kV and 40 mA. The 2θ range was 5–70° with a step size of 0.02°, and a step time of 1 s. The structures of the reported materials were refined using the Rietveld method with the GSAS program.[8] The refinements of the solid-solutions were carried out in the NCS space group, $P2_1am$ (No. 26) with a starting model of the reported neutron diffraction data of $CsBiNb_2O_7$.[7a] With the $CsBi_{1-x}Eu_xNb_2O_7$ (x = 0.1 and 0.2) solid solutions, the Bi^{3+} and Eu^{3+} cations were statistically disordered over the unique Bi^{3+} site in $CsBiNb_2O_7$. Attributable to the layered nature of the materials, a strong preferred orientation in the [001] plane was observed from the diffraction data. Thus, the amount to preferential orientation was refined using the March-Dollase function in the GSAS program. The crystallographic data and refinement results for $CsBi_{1-x}Eu_xNb_2O_7$ (x = 0, 0.1, 0.2) are summarized in Table 1. Atomic coordinates and isotropic displacement parameters for the reported materials can be found in the ESI.

Table1 Summary of crystallographic data and refinement results for $CsBi_{1-x}Eu_xNb_2O_7$ (x = 0, 0.1, 0.2)

x	0	0.1	0.2
fw	639.69	633.99	628.29
Space group	$P2_1am$	$P2_1am$	$P2_1am$
a/Å	5.5076(3)	5.49965(17)	5.49383(18)
b/Å	5.4338(3)	5.42665(17)	5.41868(18)
c/Å	11.4006(3)	11.3596(2)	11.3158(3)
V/Å^3	341.19(3)	339.022(16)	336.863(18)
Z	2	2	2
R_p [a]	0.1082	0.0789	0.0790
R_{wp} [b]	0.1474	0.1034	0.1055

[a] $R_p = \Sigma |I_o - I_c| / \Sigma I_o$. [b] $R_{wp} = [\Sigma w |I_o - I_c|^2 / \Sigma w I_o^2]^{1/2}$.

Infrared (IR) spectroscopy

Infrared spectra for the solid solutions were recorded on a Thermo Scientific Nicolet 6700 FT-IR spectrometer in the 400–4000 cm^{-1} range, with the samples embedded in KBr matrixes.

UV-vis diffuse reflectance spectroscopy

UV-vis diffuse reflectance spectra were obtained on a Varian Cary 500 scan UV-vis-NIR spectrophotometer over the spectral range 200–2500 nm at room temperature. The reflectance spectra were transformed to the absorbance using the Kubelka-Munk function.[9]

Second-harmonic generation (SHG) Measurements

Powder SHG measurements on polycrystalline $CsBi_{1-x}Eu_xNb_2O_7$ were performed on a modified Kurtz-NLO system[10] using 1064 nm radiation. A DAWA Q-switched Nd:YAG laser, operating at 20 Hz, was employed for the measurements. Because SHG efficiency is strongly depend on particle size, polycrystalline samples were sieved (Newark Wire Cloth Co.) into distinct particle size ranges (20–45, 45–63, 63–75, 75–90, 90–125, 125–150, 150–200, >250 μm). To compare with known SHG materials suitably, polycrystalline α-SiO_2 and $LiNbO_3$ were also sieved into the same particle size ranges. Samples with particle size 45–63 μm were used for comparing SHG efficiencies. All of the sieved samples with different particle sizes were packed into distinct capillary tubes. The reflected green SHG light with 532 nm was collected and detected by a photomultiplier tube (Hamamatsu). To detect only the SHG light, a 532 nm narrow band-pass interference filter was attached to the front of the tube. The generated SHG signal was monitored using a digital oscilloscope (Tektronix TDS1032). A detailed description of the methodology and the equipment used has been previously published.[1g]

Results and discussion

Crystal structure description

Since the structure of $CsBiNb_2O_7$ has been determined through powder neutron diffraction,[7a] a brief structural description will be provided. As a Dion-Jacobson phase with the general composition of $A'A_{n-1}B_nO_{3n+1}$, $CsBiNb_2O_7$ exhibits a layered perovskite structure. $CsBiNb_2O_7$ crystallizes in a noncentrosymmetric polar space group, $P2_1am$ (No. 26) at room temperature. As seen in Fig. 1, the structure of $CsBiNb_2O_7$ consists of corner-shared distorted NbO_6 octahedra and the A-cation, Bi^{3+}. Attributable to the displacement of Bi^{3+} cations, octahedral tilting and distortion are observed from NbO_6 octahedra. The perovskite blocks are also separated by a layer of metal cation, Cs^+ (see Fig. 1). The distortion of NbO_6 octahedra occurs toward a corner (local C_4 direction), which results in one short, one long, and four intermediate Nb–O bonds. In order to explore the origin of SHG and luminescent properties of $CsBiNb_2O_7$, the A-site cation with the lone pair,

Journal of Materials Chemistry C Accepted Manuscript

This journal is © The Royal Society of Chemistry 2012

Bi^{3+} has been replaced by the rare earth metal cation, Eu^{3+}. In other words, up to 20% of Eu^{3+} cation has been substituted for the A-cation, Bi^{3+} to form solid solutions, *i.e.*, $CsBi_{1-x}Eu_xNb_2O_7$ (x = 0.1 and 0.2). Fig. 2 reveals the powder X-ray diffraction patterns for solid solutions of $CsBi_{1-x}Eu_xNb_2O_7$. As seen in Fig. 2, the peak positions slightly shift toward right-hand side as more Eu^{3+} cations are doped to the Bi^{3+} positions. The peak shift is attributed to the smaller ionic radius of Eu^{3+} compared to that of Bi^{3+}. The ionic radii of eight-coordinate Eu^{3+} and Bi^{3+} are 1.066 and 1.17 Å, respectively. The difference in ionic radii of the cations significantly influences the lattice constants and the unit-cell volumes. As can be seen in Fig. 3, the unit-cell parameters and the cell volumes decrease with increasing Eu^{3+} on the Bi^{3+} site.

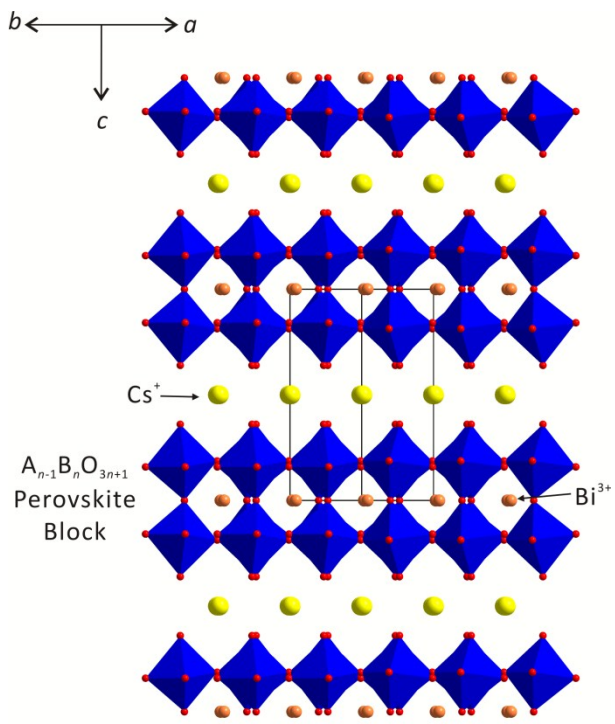

Fig. 1 Ball-and-stick and polyhedral representation of $CsBiNb_2O_7$ viewed along the [110] direction. The Dion-Jacobson phase consists of $A_{n-1}B_nO_{3n+1}$ perovskite blocks and layers of A' cation (blue, Nb; orange, Bi; yellow, Cs; red, O).

The experimental, calculated, and difference X-ray diffraction plots for $CsBi_{0.8}Eu_{0.2}Nb_2O_7$ are shown in Fig. 4 with the refinement results given in Table 1. Final Rietveld plots along with atomic coordinates and displacement parameters for all other solid solutions are shown in the ESI.

Infrared (IR) spectroscopy

The infrared spectra for $CsBiNb_2O_7$, $CsBi_{0.9}Eu_{0.1}Nb_2O_7$, and $CsBi_{0.8}Eu_{0.2}Nb_2O_7$ reveal Nb–O and Bi–O vibrations. Broad bands at ca. 580–590 cm^{-1} and strong peaks at ca. 913–919 cm^{-1} are attributable to Nb–O and Nb=O vibrations, respectively. Bi–O vibrations are also observed around 479–490 cm^{-1}. It should be noticed that as Eu^{3+} is added to the site of Bi^{3+}, the Bi–O vibration peaks are getting broader with coming into existence of Eu–O bonds. The IR vibrations are consistent with those previously published materials.[11] The IR spectra for $CsBi_{1-x}Eu_xNb_2O_7$ solid solutions are found in the ESI.

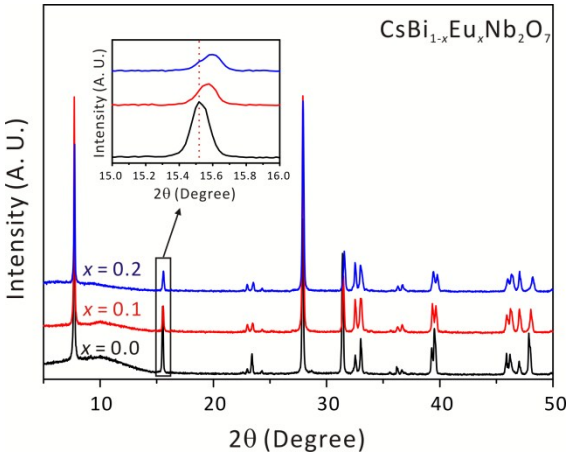

Fig. 2 Powder X-ray diffraction patterns for $CsBi_{1-x}Eu_xNb_2O_7$ (x = 0, 0.1, and 0.2). Note the peak positions shift toward right-hand side as the x increases.

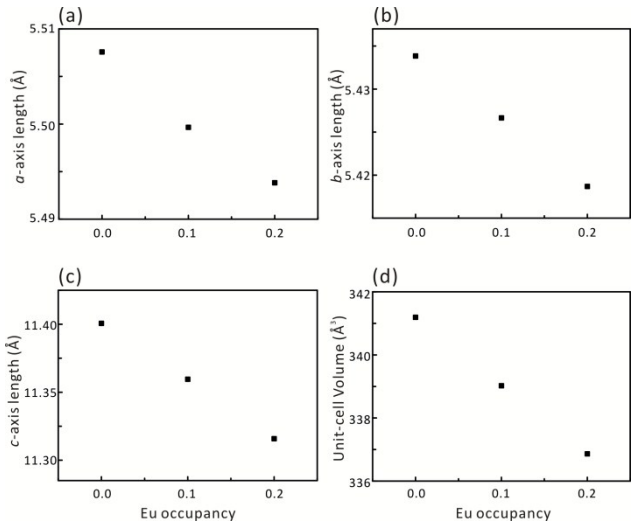

Fig. 3 Variation of the lattice parameters as a function of the Eu occupancy for $CsBi_{1-x}Eu_xNb_2O_7$ solid solution. (a) the a-axis, (b) the b-axis, (c) the c-axis, and (d) the unit-cell volume.

UV-vis reflectance spectroscopy

The UV-vis diffuse reflectance spectra for $CsBi_{1-x}Eu_xNb_2O_7$ (x = 0, 0.1, and 0.2) have been measured and absorption (K/S) data were calculated from the following Kubelka-Munk function:[9]

$$F(R) = \frac{(1-R)^2}{2R} = \frac{K}{S}$$

Journal of Materials Chemistry C Accepted Manuscript

where K is the absorption, S is the scattering, and R is the reflectance. Once the linear parts of the ascending curves are extrapolated to zero, the onsets of absorptions are observed at ca. 3.4 eV in the (K/S)-vs-E plots for $CsBiNb_2O_7$ and $CsBi_{0.9}Eu_{0.1}Nb_2O_7$. The onset of optical absorption has slightly decreased and is monitored at ca. 3.3 eV for $CsBi_{0.8}Eu_{0.2}Nb_2O_7$. The band gaps for the solid solutions may be attributable to the distortions arising from the polyhedra of A-site cation, Bi^{3+}. The (K/S)-vs-E plots for $CsBi_{1-x}Eu_xNb_2O_7$ solid solutions have been included in the ESI.

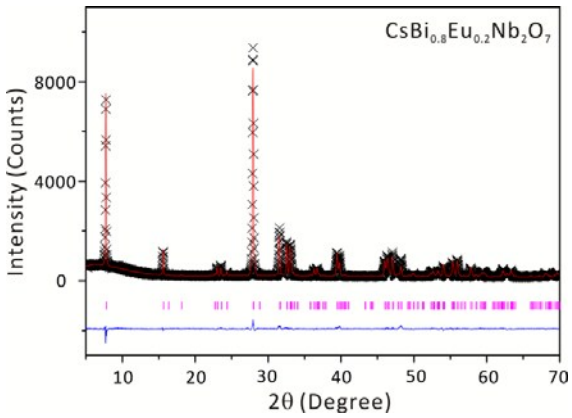

Fig. 4 Final Rietveld plot of an example $CsBi_{0.8}Eu_{0.2}Nb_2O_7$. The observed data (×) are compared with the calculated pattern (red solid line). The positions of reflections are represented by the magenta vertical bars. The difference between the observed and calculated profiles is shown at the bottom (blue solid line).

Second-order nonlinear optical (NLO) measurements

$CsBi_{1-x}Eu_xNb_2O_7$ crystallize in the noncentrosymmetric (NCS) space group, $P2_1am$; thus, the second-harmonic generating (SHG) properties of the solid-solution were examined. Powder SHG measurements on polycrystalline $CsBiNb_2O_7$, using 1064 nm radiation, reveal that the material has SHG efficiency of about 50 times that of α-SiO_2. In addition, type I phase matching capability of $CsBiNb_2O_7$ was determined by sieving the sample into various particle sizes, ranging from 20–250 μm, and measuring the SHG as a function of particle size. As seen in Fig. 5a, $CsBiNb_2O_7$ turned out to be nonphase-matchable and can be classified as the class C category of SHG materials as defined by Kurtz and Perry.[10] As the amount of Eu^{3+} cation in $CsBi_{1-x}Eu_xNb_2O_7$ increases to x = 0.1 and 0.2, however, the SHG efficiencies decrease to 30 and 25 times that of α-SiO_2, respectively (see Fig. 5b).

Structure-SHG properties relationships

The observed magnitude of the SHG efficiencies for $CsBi_{1-x}Eu_xNb_2O_7$ solid solutions can be better understood by determining the origin and the net direction of the polarization of the materials. With $CsBi_{1-x}Eu_xNb_2O_7$ solid solutions, two SOJT cations, *i.e.*, Nb^{5+} and Bi^{3+}, may contribute toward the SHG efficiencies. First, the unique Nb^{5+} cation in NbO_6 distorted octahedra reveals a corner-type distortion along the local C_4 direction, which results in one short, one long, and four intermediate Nb–O bonds. However, the moment associated with NbO_6 effectively cancels, because the polarization on the NbO_6 ocathedra alternates between [001] and [00-1] directions (see Fig. 6a). Second, the lone pair cation, Bi^{3+} is in asymmetric coordination environment. As seen in Fig. 6b, the lone pairs on the Bi^{3+} cations point approximately toward the [-1-10] and [-110] directions. Thus, a polarization attributed to the alignment of lone pairs on Bi^{3+} cations is observed along the [100] direction, because the local dipole moment for the BiO_8 polyhedra points in the opposite direction of the lone pairs (see Fig. 6b). Therefore, a net polarization is observed along the a-axis once taking the moments as a whole, which must be responsible for the observed SHG properties of $CsBi_{1-x}Eu_xNb_2O_7$ solid solutions (see Fig. 6c). As can be seen in Fig. 5b, the SHG efficiencies of $CsBi_{1-x}Eu_xNb_2O_7$ decreases as more Eu^{3+} is doped to the sites of Bi^{3+}. The decrease in SHG is compatible with the deficiency in net moment arising from the polyhedra of Bi^{3+} cation. The net moment and the corresponding SHG efficiency will decrease as the asymmetric lone pair cation, Bi^{3+} is replaced by the nonpolarizable cation, Eu^{3+}.

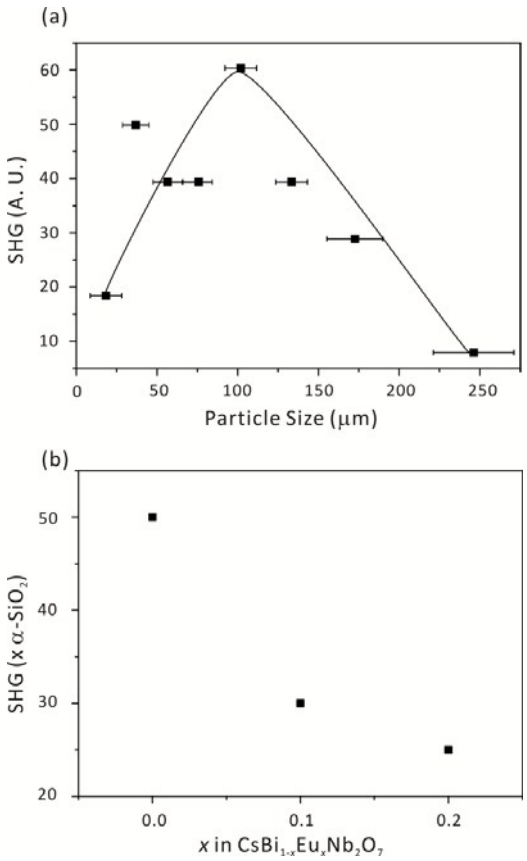

Fig. 5 (a) Phase-matching curve (Type I) for $CsBi_{1-x}Eu_xNb_2O_7$. The curve is to guide the eye and is not a fit to the data. (b) SHG *vs*. Eu^{3+} doping in $CsBi_{1-x}Eu_xNb_2O_7$. Note the SHG efficiency decrease as more Eu^{3+} is doped to the solid solutions.

Journal of Materials Chemistry C Accepted Manuscript

This journal is © The Royal Society of Chemistry 2012

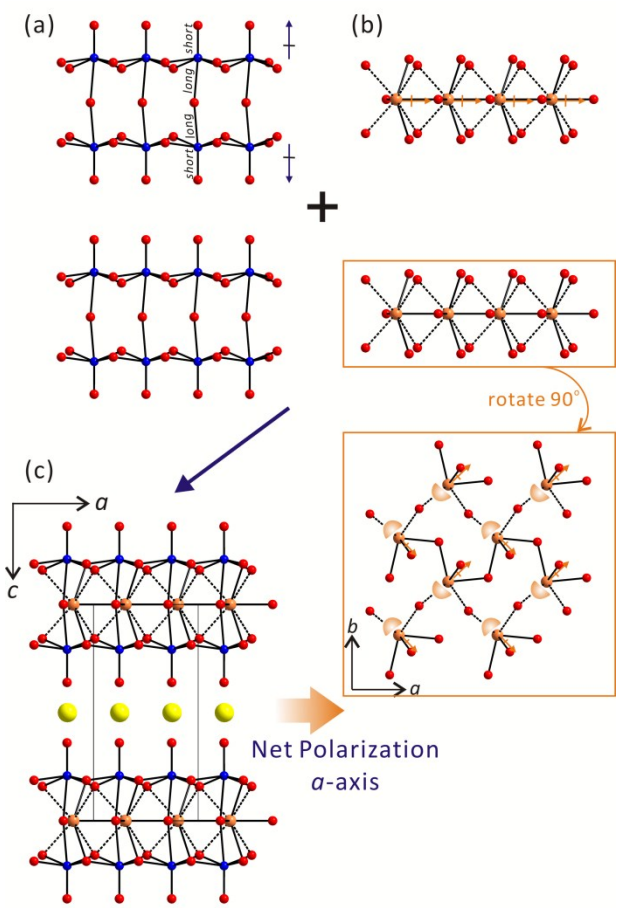

Fig. 6 Net polarization arising from the (a) Nb^{5+} cations, (b) Bi^{3+} cations, and (c) the macroscopic structure in $CsBiNb_2O_7$. While the moment associated with NbO_6 effectively cancels, that arising from the Bi^{3+} cations is observed toward the [100] direction. A net polarization is generated toward the [100] direction taking the moments as a whole.

Photoluminescence (PL) properties

Fig. 7(a) and (b) reveal the PL excitation and emission spectra for $CsBi_{1-x}Eu_xNb_2O_7$ (x = 0.1 and 0.2), respectively. Although the host material, $CsBiNb_2O_7$ does not show any band at all, $CsBi_{0.9}Eu_{0.1}Nb_2O_7$ and $CsBi_{0.8}Eu_{0.2}Nb_2O_7$ exhibit characteristic peaks attributed to the activator, Eu^{3+}. As seen in Fig. 7(a), the strong broad bands observed at ca. 330 nm in PL excitation spectra may be attributable to the charge transfer transition between oxide ligands and Eu^{3+} cations.[12] In addition, several narrow bands from characteristic f–f transitions are found ca. 378, 393, and 464 nm, which can be assigned to the $^7F_0 \rightarrow {}^5L_7$, $^7F_0 \rightarrow {}^5L_6$, and $^7F_0 \rightarrow {}^5D_2$, respectively.[13] Excitation into the charge transfer band (CTB) transition of Eu^{3+} at 330 nm yields the characteristic emission lines resulting from the transitions of $^5D_{0,1,2} \rightarrow {}^7F_j$ (j = 4, …, 0) (see Fig. 7(b)). The emission peaks observed at ca. 594, 614, and 697 nm may be attributed to the transitions, $^5D_0 \rightarrow {}^7F_1$, $^5D_0 \rightarrow {}^7F_2$, and $^5D_0 \rightarrow {}^7F_4$, respectively.[12] It has been known that luminescence peaks of Eu^{3+} in emission spectra are very sensitive to the coordination environment around Eu^{3+}.[14] If the coordination moiety of Eu^{3+} is symmetric with inversion symmetry, the f–f electric dipole transitions are strictly forbidden due to the parity selection rule. The transitions can occur when the case is only $\Delta J = 0, \pm1$ ($J = 0 \rightarrow 0$ forbidden) or vibronic electric dipole transition. Thus, the magnetic dipole $^5D_0 \rightarrow {}^7F_1$ emission transition is dominated. However, if the positions of Eu^{3+} ions do not have any inversion symmetry, *i.e.*, noncetrosymmetric, electric dipole transition can also appear. The transitions with $\Delta J = 0, \pm2$ is especially sensitive to the environment around Eu^{3+} ions. It is noticed that the electric dipole $^5D_0 \rightarrow {}^7F_2$ transition about 614 nm is stronger than the magnetic dipole $^5D_0 \rightarrow {}^7F_1$ around 594 nm in the PL emission spectra of $CsBi_{1-x}Eu_xNb_2O_7$, which clearly suggests that the environment of Eu^{3+} is asymmetric. It is consistent with the fact that Eu^{3+} cations are substituted for the asymmetric lone pair cations, Bi^{3+}, in $CsBi_{1-x}Eu_xNb_2O_7$ solid solutions.

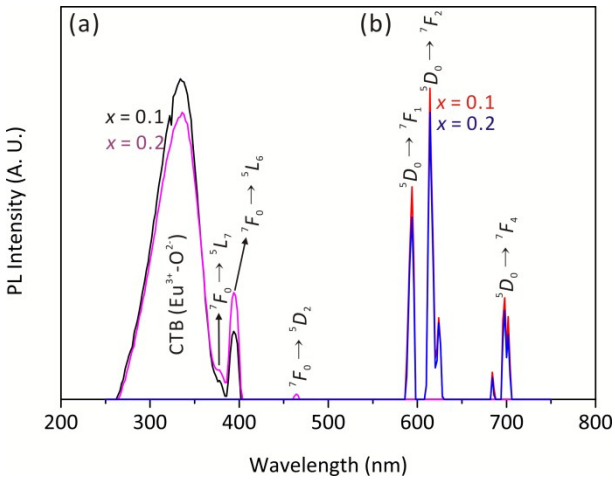

Fig. 7 (a) The PL excitation and (b) the emission spectra of $CsBi_{1-x}Eu_xNb_2O_7$ (x = 0.1 and 0.2).

Conclusions

Pure samples of Eu^{3+}-doped NCS Dion-Jacobson phase perovskite solid solutions, $CsBi_{1-x}Eu_xNb_2O_7$ (x = 0, 0.1, and 0.2) have been synthesized through standard solid-state reactions. The crystal structures of the reported materials were refined by powder X-ray diffraction using a Rietveld method. Powder second-harmonic generation (SHG) measurements on $CsBiNb_2O_7$, $CsBi_{0.9}Eu_{0.1}Nb_2O_7$, $CsBi_{0.8}Eu_{0.2}Nb_2O_7$ using 1064 nm radiation, indicate that the materials are nonphase-matchable (type I) with SHG efficiencies approximately 50, 30, and 25 times that of α-SiO_2, respectively. The SHG efficiencies of $CsBi_{1-x}Eu_xNb_2O_7$ solid solutions are mainly attributable to a net moment arising from the polyhdra of polarizable lone pair cation, Bi^{3+} on the basis of thorough structural analysis and SHG measurements. Photoluminescence (PL) excitation and emission spectra for $CsBi_{1-x}Eu_xNb_2O_7$ exhibit characteristic

Journal of Materials Chemistry C Accepted Manuscript

bands for f–f transitions. The PL emission spectra also strongly suggest the asymmetric coordination environment of Bi^{3+}/Eu^{3+} site in $CsBi_{1-x}Eu_xNb_2O_7$ solid solutions.

Acknowledgements

This work was supported by the National Research Foundation of Korea (NRF) grant funded by the Korea government (MSIP) (No. 2013R1A2A2A01007170 and 2014M3A9B8023478). This research was also supported by the Chung-Ang University Freshmen Academic Record Excellent Scholarship Grants in 2014 (for H.G.K.).

Notes and references

[a]*Department of Chemistry, Chung-Ang University, Seoul, 156-756, Republic of Korea.* [b]*School of Chemical Engineering and Materials Science, Chung-Ang University, Seoul, 156-756, Republic of Korea. Fax: 82 2 825 4736; Tel: 82 2 820 5197; E-mail: kmok@cau.ac.kr*

†Electronic Supplementary Information (ESI) available: Final Rietveld plots, atomic coordinates and isotropic displacement parameters, infrared spectra, and UV-Vis diffuse reflectance spectra for $CsBi_{1-x}Eu_xNb_2O_7$ (x = 0, 0.1, and 0.2). See DOI: 10.1039/b000000x/

1. (a) F. Jona and G. Shirane, *Ferroelectric Crystals*, Pergamon Press, Oxford, 1962; (b) W. G. Cady, *Piezoelectricity; an Introduction to the Theory and Applications of Electromechanical Phenomena in Crystals*, Dover, New York, 1964; (c) S. B. Lang, *Sourcebook of Pyroelectricity*, Gordon & Breach Science, London, 1974; (d) P. S. Halasyamani and K. R. Poeppelmeier, *Chem. Mater.*, 1998, **10**, 2753; (e) H. Schmid, *Magnetoelectric Interaction Phenomena in Crystals*, Kluwer, Dordrecht, 2004; (f) N. A. Spaldin and M. Fiebig, *Science*, 2005, **309**, 391; (g) K. M. Ok, E. O. Chi and P. S. Halasyamani, *Chem. Soc. Rev.*, 2006, **35**, 710; (h) D. I. Khomskii, *Physics*, 2009, **2**, 20; (i) S. W. Kim, H. Y. Chang and P. S. Halasyamani, *J. Am. Chem. Soc.*, 2010, **132**, 17684.
2. (a) U. Opik and M. H. L. Pryce, *Proc. R. Soc. London*, 1957, **A238**, 425; (b) R. A. Wheeler, M.-H. Whangbo, T. Hughbanks, R. Hoffmann, J. K. Burdett and T. A. Albright, *J. Am. Chem. Soc.*, 1986, **108**, 2222; (c) H.-S. Ra, K. M. Ok and P. S. Halasyamani, *J. Am .Chem. Soc.*, 2003, **125**, 7764; (d) U. V. Waghmare, N. A. Spaldin, H. C. Kandpal and R. Seshadri, *Phys. Rev. B*, 2003, **67**, 125111; (e) E. O. Chi, K. M. Ok, Y. Porter and P. S. Halasyamani, *Chem. Mater.*, 2006, **18**, 2070; (f) M. W. Stoltzfus, P. Woodward, R. Seshadri, J.-H. Park and B. Bursten, *Inorg. Chem.*, 2007, **46**, 3839; (g) H. Y. Chang, S.-H. Kim, P. S. Halasyamani and K. M. Ok, *J. Am. Chem. Soc.*, 2009, **131**, 2426; (h) C.-F. Sun, C.-L. Hu, X. Xu, J.-B. Ling, T. Hu, F. Kong, X.-F. Long and J.-G. Mao, *J. Am. Chem. Soc.*, 2009, **131**, 9486; (i) S. Zhang, H. Jiang, C. Sun and J. G. Mao, *Inorg. Chem.*, 2009, **48**, 11809; (j) B. Yang, C. Hu, X. Xu, C. Sun, H. Zhang Jian and J. G. Mao, *Chem. Mater.*, 2010, **22**, 1545; (k) C.-F. Sun, C.-L. Hu, X. Xu, B.-P. Yang and J.-G. Mao, *J. Am. Chem. Soc.*, 2011, **133**, 5561; (l) B.-P. Yang, C.-L. Hu, X. Xu, C. Huang and J.-G. Mao, *Inorg. Chem.*, 2013, **52**, 5378; (m) Y. H. Kim, D. W. Lee and K. M. Ok, *Inorg. Chem.*, 2014, **53**, 5240; (n) Y. H. Kim, D. W. Lee and K. M. Ok, *Inorg. Chem.*, 2014, **53**, 1250.
3. (a) S. Pan, J. P. Smit, B. Watkins, M. R. Marvel, C. L. Stern and K. R. Poeppelmeier, *J. Am. Chem. Soc.*, 2006, **128**, 11631; (b) Y. Inaguma, M. Yoshida and T. Katsumata, *J. Am. Chem. Soc.*, 2008, **130**, 6704; (c) H. Jiang, S. Huang, Y. Fan, J. Mao and W. Cheng, *Chem. - Eur. J.*, 2008, **14**, 1972; (d) H. Wu, S. Pan, K. R. Poeppelmeier, H. Li, D. Jia, Z. Chen, X. Fan, Y. Yang, J. M. Rondinelli and H. Luo, *J. Am. Chem. Soc.*, 2011, **133**, 7786; (e) Y. Yang, S. Pan, X. Hou, C. Wang, K. R. Poeppelmeier, Z. Chen, H. Wu and Z. Zhou, *J. Mater. Chem.*, 2011, **21**, 2890; (f) H. Yu, H. Wu, S. Pan, Z. Yang, X. Su and F. Zhang, *J. Mater. Chem.*, 2012, **22**, 9665; (g) Y. Wang, S. Pan, M. Zhang, S. Han, X. Su and L. Dong, *CrystEngComm*, 2013, **15**, 4956; (h) L. Zhou, S. Pan, X. Dong, H. Yu, H. Wu, F. Zhang and Z. Zhou, *CrystEngComm*, 2013, **15**, 3412; (i) H. Li, H. Wu, X. Su, H. Yu, S. Pan, Z. Yang, Y. Lu, J. Han and K. R. Poeppelmeier, *J. Mater. Chem. C*, 2014, **2**, 1704.
4. (a) R. E. Sykora, K. M. Ok, P. S. Halasyamani and T. E. Albrecht-Schmitt, *J. Am .Chem. Soc.*, 2002, **124**, 1951; (b) J. Goodey, K. M. Ok, J. Broussard, C. Hofmann, F. V. Escobedo and P. S. Halasyamani, *J. Solid State Chem.*, 2003, **175**, 3; (c) K. M. Ok, J. Baek, P. S. Halasyamani and D. O'Hare, *Inorg. Chem.*, 2006, **45**, 10207; (d) H.-Y. Chang, S.-H. Kim, K. M. Ok and P. S. Halasyamani, *J. Am. Chem. Soc.*, 2009, **131**, 6865; (e) M.-H. Choi, S.-H. Kim, H. Y. Chang, P. S. Halasyamani and K. M. Ok, *Inorg. Chem.*, 2009, **48**, 8376; (f) D. W. Lee, D.-b. Bak, S. B. Kim, J. Kim and K. M. Ok, *Inorg. Chem.*, 2012, **51**, 7844; (g) S.-J. Oh, D. W. Lee and K. M. Ok, *Inorg. Chem.*, 2012, **51**, 5393; (h) D. W. Lee and K. M. Ok, *Inorg. Chem.*, 2013, **52**, 5176; (i) S. Han, Y. Wang, S. Pan, X. Dong, H. Wu, J. Han, Y. Yang, H. Yu and C. Bai, *Cryst. Growth Des.*, 2014, **14**, 1794; (j) Y. H. Kim, T. T. Thao, P. S. Halasyamani and K. M. Ok, *Inorg. Chem. Front.*, 2015, DOI: 10.1039/C1034QI00243A.
5. (a) A. J. Jacobson, J. W. Johnson and J. T. Lewandowski, *Mater. Res. Bull.*, 1987, **22**, 45; (b) Y. Moritomo, A. Asamitsu, H. Kuwahara and Y. Tokura, *Nature*, 1996, **380**, 141; (c) P. D. Battle, M. A. Green, N. S. Laskey, J. E. Millburn, L. Murphy, M. J. Rosseinsky, S. P. Sullivan and J. F. Vente, *Chem. Mater.*, 1997, **9**, 552; (d) S. Ikeda, A. Tanaka, M. Hara, J. N. Kondo, K. Maruya and K. Domen, *Microporous Mater.*, 1997, **9**, 253; (e) R. Seshadri, C. Martin, M. Herien, B. Raveau and C. N. R. Rao, *Chem. Mater.*, 1997, **9**, 270; (f) T. Wang, C. N. Henderson, T. I. Draskovic and T. E. Mallouk, *Chem. Mater.*, 2013, **26**, 898.
6. S.-J. Oh, Y. Shin, T. T. Tran, D. W. Lee, A. Yoon, P. S. Halasyamani and K. M. Ok, *Inorg. Chem.*, 2012, **51**, 10402.
7. (a) A. Snedden, K. S. Knight and P. Lightfoot, *J. Solid State Chem.*, 2003, **173**, 309; (b) F. Lichtenberg, A. Herrnberger and K. Wiedenmann, *Prog. Solid State Chem.*, 2008, **36**, 253; (c) C. Chen, H. Ning, S. Lepadatu, M. Cain, H. Yan and M. J. Reece, *J. Mater. Chem. C*, 2015, **3**, 19.
8. A. C. Larson and R. B. von Dreele, *General Structural Analysis System (GSAS)*, Los Alamos National Laboratory, Los Alamos, NM, 1987.
9. (a) P. Kubelka and F. Munk, *Z. Tech. Phys.* , 1931, **12**, 593; (b) J. Tauc, *Mater. Res. Bull.*, 1970, **5**, 721.
10. S. K. Kurtz and T. T. Perry, *J. Appl. Phys.*, 1968, **39**, 3798.
11. (a) Y.-S. Han, I. Park and J.-H. Choy, *J. Mater. Chem.*, 2001, **11**, 1277; (b) S. D. Nguyen, J. Yeon, S.-H. Kim and P. S. Halasyamani, *J.*

Journal of Materials Chemistry C Accepted Manuscript

This journal is © The Royal Society of Chemistry 2012

Am. Chem. Soc., 2011, **133**, 12422; (c) H. Jo, Y. H. Kim, D. W. Lee and K. M. Ok, *Dalton Trans.*, 2014, **43**, 11752.
12. D. Geng, G. Li, M. Shang, C. Peng, Y. Zhang, Z. Cheng and J. Lin, *Dalton Trans.*, 2012, **41**, 3078.
13. (a) P. Dorenbos, *J. Lumin.*, 2005, **111**, 89; (b) X. Liu, C. K. Lin and J. Lin, *Appl. Phys. Lett.*, 2007, **80**, 081904; (c) P. Dorenbos, *J. Alloys Compd.*, 2009, **488**, 568.
14. G. Blasse and B. C. Grabmaier, *Luminescent Materials*, Springer-Verlag, Berlin, 1994.

Journal of Materials Chemistry C Accepted Manuscript

A graphical contents entry:

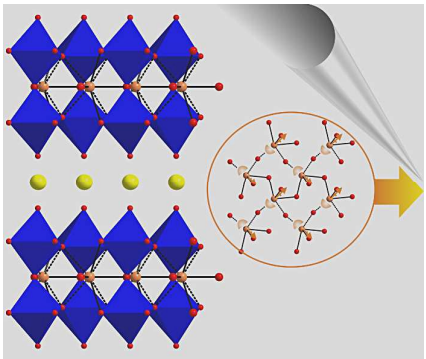

A series of solid solutions of noncentrosymmetric (NCS) Dion-Jacobson phases, $CsBi_{1-x}Eu_xNb_2O_7$ (x = 0, 0.1, and 0.2) have been synthesized by standard solid-state reactions. The added foreign cation, Eu^{3+}, not only indicates the asymmetric coordination sites for the associated SHG properties, but also promises important applications to novel phosphor materials.

Journal of Materials Chemistry C Accepted Manuscript